IEEE Access
Multidisciplinary | Rapid Review | Open Access Journal

Received November 7, 2021, accepted December 1, 2021, date of publication December 8, 2021,
date of current version December 20, 2021.

Digital Object Identifier 10.1109/ACCESS.2021.3134166

Optimizing Seizure Prediction From Reduced Scalp EEG Channels Based on Spectral Features and MAML

ANIBAL ROMNEY[1], (Member, IEEE), AND VIDYA MANIAN[2], (Member, IEEE)
[1]Department of Bioengineering, University of Puerto Rico at Mayagüez, Mayagüez, PR 00682, USA
[2]Department of Electrical and Computer Engineering, University of Puerto Rico at Mayagüez, Mayagüez, PR 00682, USA
Corresponding author: Anibal Romney (anibal.romney@upr.edu)

ABSTRACT Epilepsy is a severe neurological disease with high prevalence and morbidity worldwide. The unpredictability of seizures prevents physicians from tailoring drugs and therapies. Recent non-invasive seizure prediction research has not improved the overall quality of life for patients. Therefore, new research studies on seizure prediction must integrate data, embedded devices, and algorithms. For a seizure prediction system to emerge as a feasible solution, we must address a reduction in EEG scalp electrode channels, along with a decrease in computational resources to train the time-series signal. In this work, we propose an optimized patient-specific channel reduction for seizure prediction using Model Agnostic Meta-Learning (MAML) applied to a Deep Neural Network (DNN). We selected and optimized the number of channels from each of the 23 subjects of the CHB-MIT Dataset. The feature vectors are extracted using Ensemble Empirical Mode Decomposition (EEMD) and Sequential Feature Selection (SFS). We implemented the MAML model to classify the small EEG data generated from the reduced number of subject-dependent electrodes. The experiment results yield an average sensitivity and specificity of 91% and 90%, respectively. Our study demonstrates that MAML is a promising approach to learn EEG patterns to predict epileptic seizures with few EEG scalp electrodes.

INDEX TERMS Seizure prediction, channels reduction, scalp EEG, preictal state, MAML.

I. INTRODUCTION

Epilepsy is a severe neurological disorder whose central aspect is the recurrence of seizure episodes [1]–[3]. The unpredictability of seizures and the accompanying symptoms, including unusual behavior, sudden falling, jerking movements, and altered consciousness [4], [5], make the condition unbearable for the patient and difficult to manage. Seizures are triggered by the synchronous activation of millions of neurons that generate an action potential or spike that propagates partially or entirely through the brain's cortex [6]. The epileptiform generated during seizure onset is recorded by an electroencephalogram (EEG), a gold standard in the field of neuroscience. This signal has four stages: interictal, preictal, ictal, and postictal [8]. Surgery, antiepileptic drugs, and vagus nerve stimulation are the leading therapies for epileptic seizures [7]–[9]. Physicians currently prescribe neuro-stimulation therapies and drug regimens without a monitoring signal to modulate or adapt treatment in response to physiological changes during seizure onset [10]. An algorithm that overcomes the unpredictable aspect of seizures in real-time would allow the physician to design a therapeutic and pharmacological solution tailored to the patient [11]. Regardless of the advances in non-invasive seizure prediction over the past decades, a real-time seizure prediction that would significantly impact patients' quality of life has yet to be accomplished [12]–[17]. For a real-time wearable seizure prediction system to become a realistic alternative for patients, the number of scalp electrode channels must be reduced to obtain better patient handling and acceptance while decreasing preprocessing and algorithm training. Also, the number of channel electrodes should be patient-specific based on the type and location of seizure. Some of the most recent research on seizure prediction uses patient-specific modeling but with a global EEG electrodes selection [18]–[20]. The patient-specific channel reduction would generate a short data set for training and testing. The model-agnostic meta-learning (MAML)

The associate editor coordinating the review of this manuscript and approving it for publication was Cesar Vargas-Rosales.

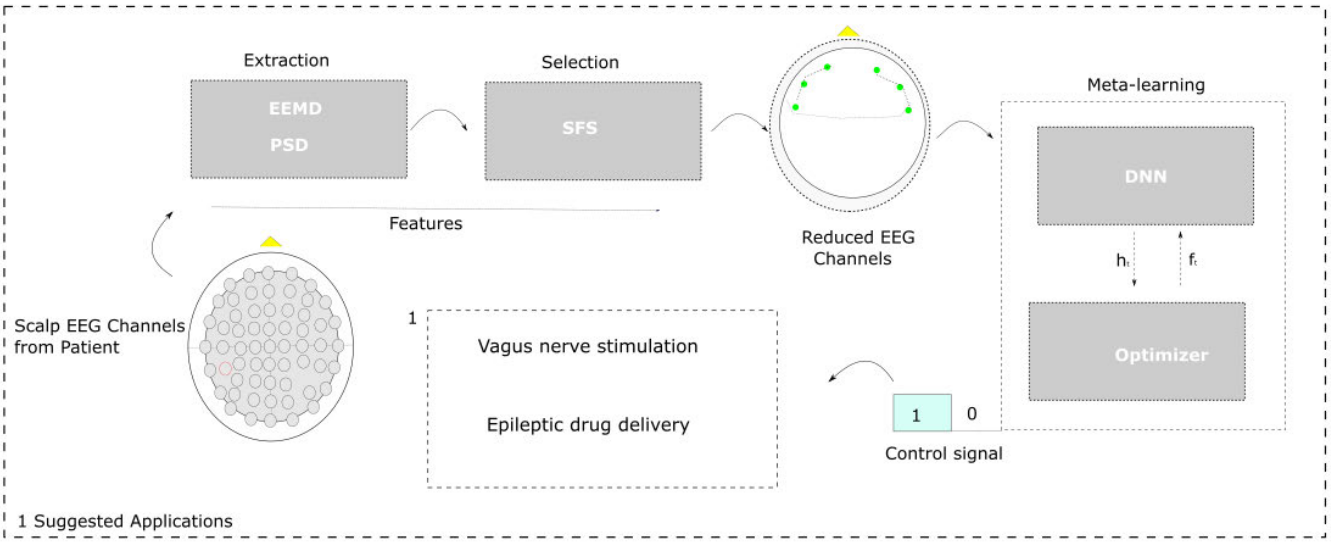

FIGURE 1. The proposed model implemented on each of the 23 patient EEG recordings.

algorithm works effectively on small data, although it has not yet been implemented in seizure prediction. The most advanced machine learning methods, including deep neural networks, have helped improve the learning process, but with little success in training small data sets [21], [22], [16]. To tackle all constraints mentioned above, we implemented patient-specific channel reduction, feature-engineering, and MAML algorithm for a high sensitivity and specificity seizure prediction. We use MAML to train a model on various training activities to solve new learning tasks using only a few training samples [16], [23]. Figure 1 shows the proposed general model. The MAML algorithm is applied to a DNN to train an optimized number of personalized electrode-channel features from each subject to learn preictal signatures.

This study's main contributions are summarized as follows:

- This work presents the first seizure prediction model on patient-specific electrode channels trained with a MAML algorithm on a deep neural network.
- This model is suitable for a wearable seizure prediction device on a patient-specific electrode channels selection.
- We improve seizure prediction portability by combining a personalized electrode channels and a low data algorithm applied on each patient.

We organize the remaining sections of this work as follows. Section II provides related work on seizure prediction. In Section III, we present the methodology. Section IV provides results and discussion. Finally, conclusions are given in Section V.

II. EPILEPTIC SEIZURE PREDICTION

Many researchers have addressed the problem of seizure prediction over the past four decades. Many authors have developed multiple feature extraction and classification methods and applied them to the epileptiform EEG time-series signal. However, a great interest in seizure prediction has increased in recent years because of new mathematical analyses, modern machine learning algorithms, and a better understanding of the preictal state in the scalp EEG signal. Currently, the most proposed seizure prediction methods based on machine learning include Support Vector Machine (SVM), Bayesian Gaussian, Random Forest, Logistic Classifier, and XGBoost [24], [25], [10]. Support Vector Machine has demonstrated superior success with high sensitivity. Al Ghayab *et al.* [20] proposed simple random sampling (SRS) techniques to extract features from the time domain. The least-square SVM classifier used the selected six features to predict between healthy and epileptic subjects with 96.62% sensitivity. Hosseini *et al.* [26] reported a cloud-based pervasive data collection for automatic and real-time seizure detection with a wavelet transform to extract features from the frequency bands. Contrary to the previous work, they developed multiple algorithms based on ensemble learning and randomness and achieved better predictions using a SVM. The cross-validation and sensitivity of the proposed method yielded 95% and 94%, respectively. These results are remarkable but have not yet been applied to reduced electrode channels on patient-specific data.

Algorithms based on neural networks have recently gained ground in seizure prediction [9], [18]. The most widely used of these is the convolutional neural network. Nejedly *et al.* [27] developed a CNN for automated artifact detection. The method provides independent detections for each separate channel and generates an artifact probability matrix (APM). A more improved CNN application in seizure prediction is presented in Eberlein *et al.* [28]. Unlike the previous method, binary classification is conducted without handcrafted feature extraction. CNN is used for unsupervised

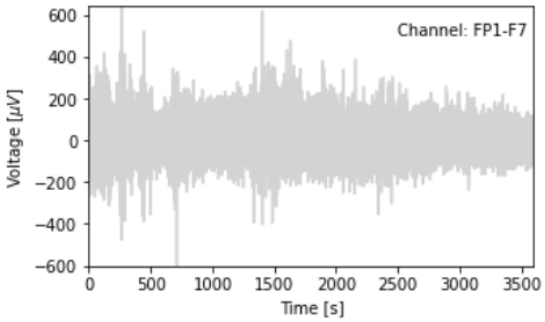

FIGURE 2. Sample EEG signal for subject S01.

feature extraction. A similar approach is used with the deep learning prediction model in Daoud and Bayoumi [9], where the raw data is directly fed after segmentation to the Multi-layer Perception to classify between preictal and interictal.

Meta-learning can optimize deep neural networks performance. The concept behind meta-learning is to learn a general-purpose algorithm by generalizing across tasks and allowing each new task to be learned better than the previous one. The concept behind meta-learning is to learn a general purpose algorithm by generalizing across tasks and allowing each new task to be learned better than the previous one [29], [30]. Meta-learning represents the process of generalized learning, in which the learning is done with few examples, just as humans learn new concepts and skills faster and efficiently. Finn *et al.* [31] proposed an algorithm for meta-learning that is model-agnostic and compatible with any gradient-trained model. In this study, the model parameters are explicitly trained, so a few gradient steps with a small training data set would produce a good generalization performance on a new task. Sucholutsky and Schonlau [32] presented a one-shot learning, where the model must learn a new class from one example. The model must learn N new classes given only M $<$ N examples. They generalize the nearest neighbor classifier soft label k to implement the algorithm in different learning scenarios.

A common limitation of previous methods is the lack of a patient-specific EEG electrode selection design, where the number and location of EEG electrodes may differ for each patient. Also, most methods elude a meta-learning approach to cope with a low patient-specific data set. Other aspects of improving seizure prediction research are maximizing sensitivity, specificity, false-positive rate, and extending the prediction horizon time.

III. MATERIALS AND METHODS

The EEG dataset from the Children's Hospital Boston and the Massachusetts Institute of Technology [33] is used to validate the proposed method. The dataset consists of EEG recordings from pediatric subjects with intractable seizures. The international 10–20 electrode positions system is used in the recordings. Table 1 shows the 23 channels and their location in the scalp EEG from recording using European

TABLE 1. 23 scalp EEG channels in the CHB-MIT recordings.

1	2	3	4	5	6
FP1-F7	F7-T7	T7-P7	P7-O1	FP1-F3	F3-C3
7	8	9	10	11	12
C3-P3	P3-O1	FP2-F4	F4-C4	C4-P4	P4-O2
13	14	15	16	17	18
FP2-F8	F8-T8	T8-P8	P8-O2	FZ-CZ	CZ-PZ
19	20	21	22	23	
P7-T7	T7-FT9	FT9-FT10	FT10-T8	T8-P8	

Data Format (EDF) files. Table 2 shows the CHB-MIT dataset, collected from 23 subjects (5 males, ages 3–22 and 17 females, ages 1.5– 19). The sampling rate of the recording is 256 Hz. We conduct preprocessing, feature extraction, feature selection, and seizure prediction from each subject's raw EEG signal.

A. PREPROCESSING

We apply to the time series EEG signal a 6th order band-pass Butterworth filter ranging from 2.5 Hz to 40 Hz to remove power harmonics, noise, and muscle artifacts. Figure 1 shows a sample EEG signal from channel FP1-F7 of subject S01. The amplitude is in μV and the time in seconds.

B. FEATURES EXTRACTION AND SELECTION

We extract features using two algorithms with demonstrated success in biomedical signal processing [34]: the empirical mode decomposition (EMD) and the power spectral density (PSD). The EMD decomposes the data x (t) into intrinsic mode functions (IMFs) represented by *cj* and the residue (*r*) of the data after the last component. The original equation introduced by Huang *et al.* [35] is shown below:

$$\boldsymbol{x}(\boldsymbol{t}) = \sum_{\boldsymbol{j}=\boldsymbol{1}}^{\boldsymbol{n}} \boldsymbol{c_j} + \boldsymbol{r_n}$$

An improvement over the original EMD is the ensemble empirical mode decomposition (EEMD) proposed by Wu and Huang [36]. EEMD uses the white noise characteristics to perturb the signal in its true solution neighborhood and cancel itself out once it has served its purpose. The algorithm adds a different set of white noise to the signal in several iterations, allowing better scale separation. Algorithm 1 formulates the ensemble EMD as follows:

The spectrum reveals important aspects of a time series signal [25]. The PSD is defined as the discrete–time Fourier transform of the covariance sequence:

$$\varphi(\omega) = \sum_{k=-\infty}^{\infty} r(k)\, e^{-iwk}$$

Algorithm 1 : Ensemble Empirical Mode Decomposition

1) add a white noise series to the targeted data;
2) decompose the data with added white noise into IMFs;
3) repeat step 1 and step 2 again and again, but with different white noise series each time; and
4) obtain the (ensemble) means of corresponding IMFs of the decompositions as the result.

TABLE 2. CHB-MIT dataset.

Subject	Gender	Age	Total Seizures	EDF Files
S01	F	11	7	43
S02	M	11	3	35
S03	F	14	7	38
S04	M	22	3	43
S05	F	7	5	3
S06	F	1.5	7	24
S07	F	14.5	3	19
S08	M	3.5	5	29
S09	F	10	3	19
S10	M	3	7	33
S11	F	12	3	38
S12	F	2	13	42
S13	F	3	8	42
S14	F	9	7	32
S15	M	16	14	53
S16	F	7	5	19
S17	F	12	3	20
S18	F	18	6	36
S19	F	19	3	30
S20	F	6	6	29
S21	F	13	4	33
S22	F	9	3	34
S23	F	6	3	9

We can recover $r\,(k)$ from a given $\varphi\,(\omega)$ as

$$r\,(k) = \frac{1}{2\pi}\int_{-\pi}^{\pi} \varphi\,(\omega)\, e^{-i\omega k} d\omega$$

We implement feature selection based on the sequential forward selection (SFS) algorithm, a wrapper-based feature selection method, which means it uses a machine-learning algorithm to select a subset of the most relevant attributes

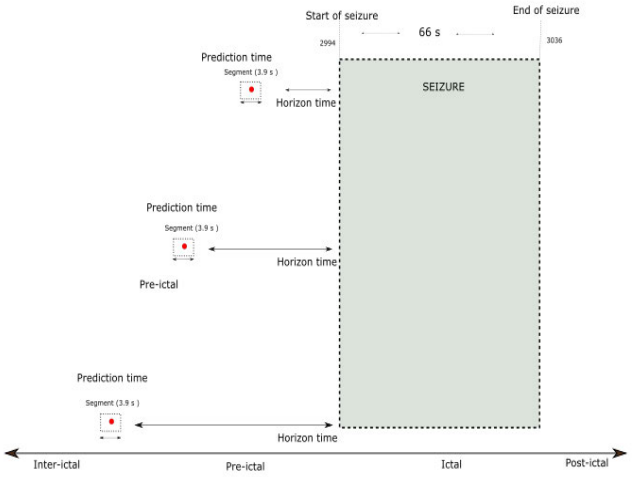

FIGURE 3. Prediction and horizon times for subject S01.

TABLE 3. Performance metrics in seizure prediction.

Measures	Computation
Accuracy-The number of correct predictions from all predictions made.	$\frac{TP+TN}{TP+TN+FP+FN}$
Sensitivity- True positive rate (TPR) of a test.	$\frac{TP}{TP+FN}$
Specificity- True negative rate (TNR) of a test	$\frac{TN}{TN+FP}$
False positive rate (FPR)	$\frac{FP}{FP+TN}$
False positive rate per hour (FPR/h).	(FPR/h) is calculated in the horizon time in the ictal transition of the epileptic EEG signal
Receiver operating characteristic (ROC).	ROC is a plot of TPR (sensitivity) against FPR (1-specificity)
Where TP =True Positive, TN =True Negative, FN = False Negative, FP = False Positive	

(features) [37]. For this work, we used a linear discriminant analysis (LDA) with the SFS.

C. ELECTRODE-CHANNELS SELECTION

For each patient's recordings, the most informative and relevant electrodes are selected. Intrinsic mode functions (IMFs) are extracted from the 23 original channels using EEMD. This vector of features is then given as input to the SFS algorithm for feature selection. SFS generates a vector (V) with all 23 channels and their relevance scores sorted in descending order. From this channel vector (V), the two highest scored electrode channels are chosen (e = 2). This number is selected as the initial value since the minimum number of channels

Algorithm 2 : Model-Agnostic Learning for Fast Adaptation of Deep Networks

Given: $\rho(\tau)$: distribution over tasks
Given: α, β: step size hyperparameters
(1) randomly initialize θ
(2) **while** not done do
(3) Sample batch of tasks $\tau_i \sim \rho(\tau)$
(4) **For** all τ_i **do**
(5) Evaluate $\nabla_\theta \pounds\tau_i(f_\theta)$ with respect
(6) to K examples
(7) Compute adapted parameters
(8) with gradient descent:
(9) $\theta_i' = \theta - \alpha\nabla_\theta \pounds\tau_i(f_\theta)$
(10) **end for**

reported in the literature to support seizure prediction are two and three electrodes [38], [39]. The signal from each selected channel is discomposed to its IMFs using EEMD. The average PSD is computed for each corresponding channel IMF. These selected features are the inputs to the DNN meta-learning model. The optimal number of electrodes is attained when (sensitivity, specificity $> 90\%$); otherwise, we increase by one the number of channels with the highest score to be used in the next iteration. These steps are repeated for each patient dataset.

A model is specifically trained with each subject's recoding. The duration of a seizure varies from 10 s to 63 s. The seizure prediction horizon (SPH) is the time between the alarm and the seizure onset, as defined in [25]. We are using three SPHs of 23 min, 10 min, and 5 min, as shown in Figure 3. In each prediction horizon, we are using two overlapping windows of 3.9 seconds.

D. MAML TRAINING

We are using Model-Agnostic Meta-Learning on DNN to train the initial parameters of the model for each patient to maximize the seizure prediction performance. The parameters are updated through gradient steps computed with a small amount of data from the new task. Algorithm 2 shows the model-agnostic method [31].

A DNN with eight hidden layers is designed. We define the sigmoid activation function for output layers and the RELU activation function for input layers. The model runs with a 10% batch size and 100 epochs. We apply the Model-Agnostic algorithm to the DNN for seizure prediction in each patient data set. The feature vector is split 70% for training, and 30% for testing. All patient-specific implementation is conducted using the Python programming language.

E. PREDICTION PERFORMANCE METRICS

Accuracy measure falls short to determine the performance of the seizure prediction model; hence, four additional indicators (sensitivity, specificity, AUC-ROC, and false positive rate per hour) are employed to evaluate the performance of the prediction model [10], [40], which are calculated in Table 3.

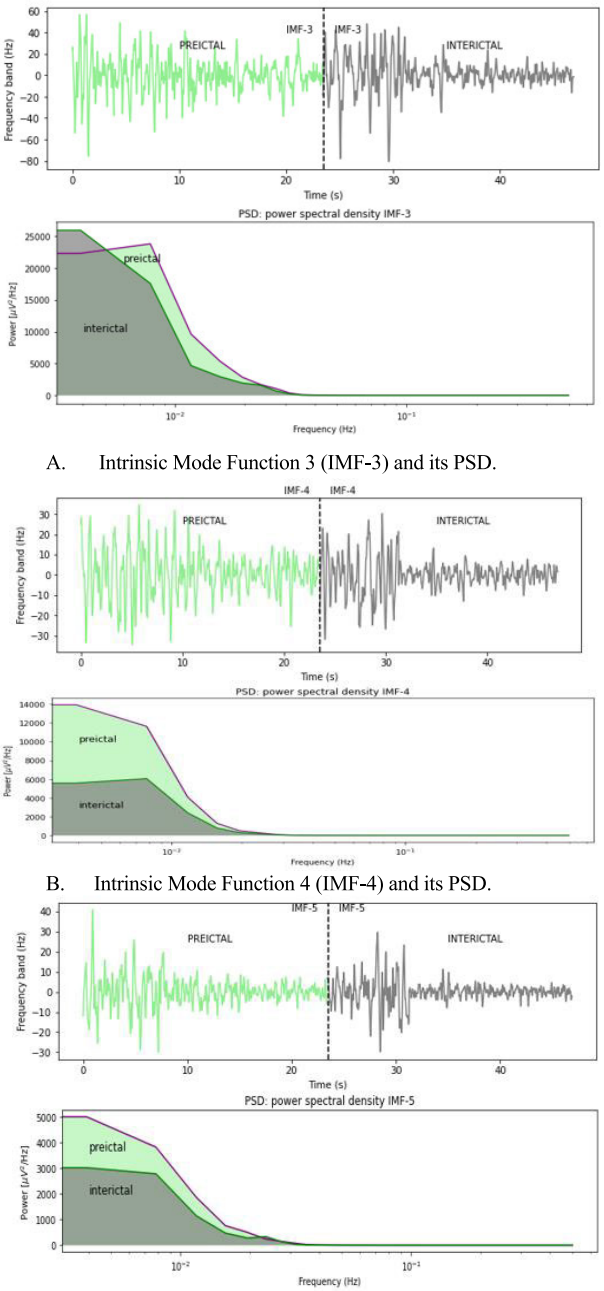

A. Intrinsic Mode Function 3 (IMF-3) and its PSD.

B. Intrinsic Mode Function 4 (IMF-4) and its PSD.

C. Intrinsic Mode Function 5 (IMF-5) and its PSD.

FIGURE 4. PSD of the intrinsic mode functions during the preictal and interictal transitions for subject S01. A) IMF-3 and its PSD, B) IMF-4 and its PSD, and C) IMF-5 and its PSD.

IV. RESULTS AND DISCUSSION

For each subject trial EEG signal, the intrinsic mode functions (IMFs) and their corresponding power spectra density are extracted in the preictal and interictal states of the epileptiform. Figure 4 shows the extracted IMF_3, IMF_4, and IMF_5 using the EEMD algorithm in the preictal and interictal segments of subject S01. Table 4 and Table 5 show a higher

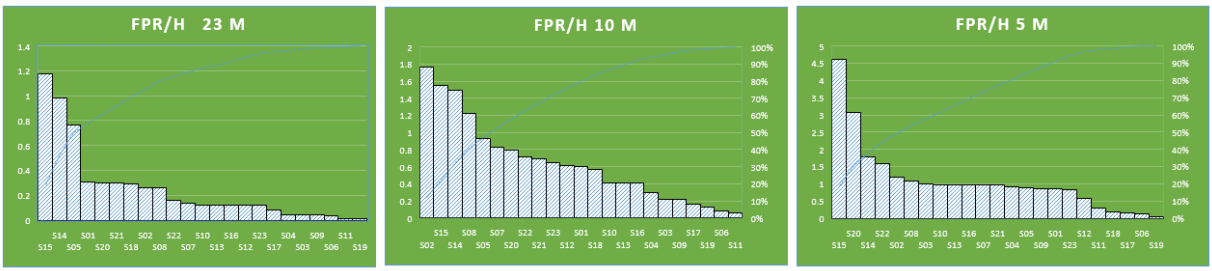

FIGURE 9. False positive rate per hour for each of the 23 subjects in different horizon times. A) 23 minutes, B) 10 minutes, and C) 5 minutes.

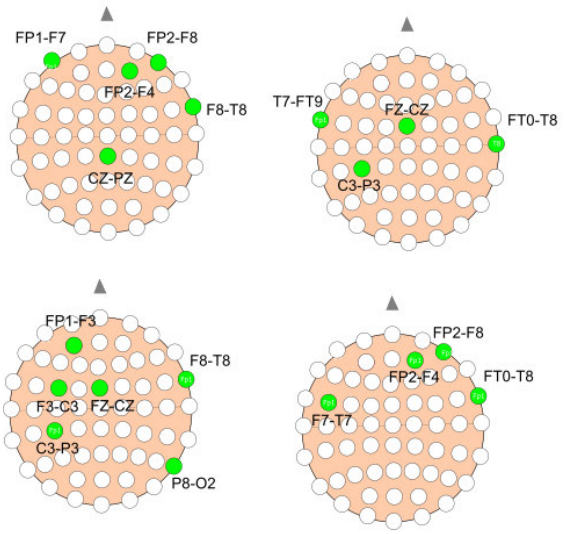

FIGURE 5. Optimal number of scalp EEG channel electrodes for subject S_{01}, S_{02}, S_{03} and S_{04}.

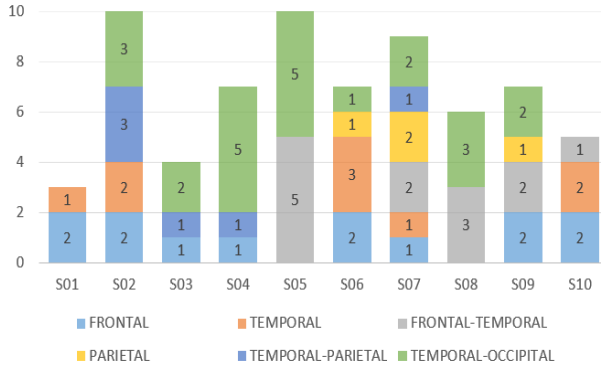

FIGURE 6. Channel location and distribution per brain lobes area.

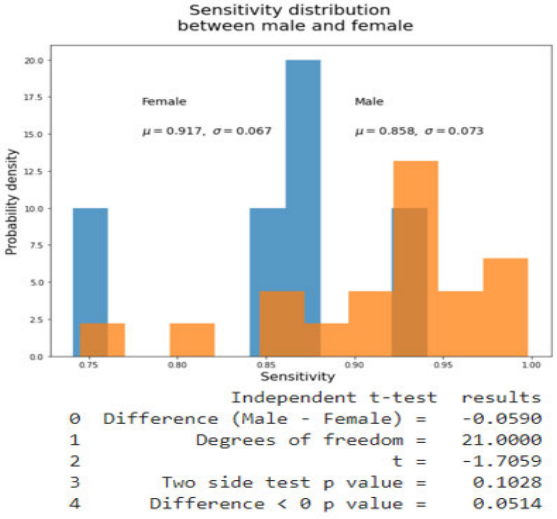

FIGURE 7. Sensitivity distribution between male and female subjects and an independent t-test result.

TABLE 4. Extracted features during the preictal frame of subject S_{01}.

Extracted Features	IMF_3	IMF_4	IMF_5
Maximum	57.226	34.568	40.408
Minimum	-75.928	-35.004	-29.250
Mean	-0.089	0.117	0.057
Standard deviation	16.588	11.396	7.218
Coefficient of Var.	-18551.2	9671.6	12452.7
Avg PSD(V^2/Hz)	548.246	269.260	106.668

average PSD of the oscillatory IMFs in the preictal than the corresponding interictal state.

The power spectral density of the intrinsic mode functions IMF_3, IMF_4, and IMF_5 extracted from the preictal and interictal segments is computed for each of the three prediction horizon times. Figure 4 shows a higher power density of the oscillatory components of the preictal state of the IMF_5.

These signature features contribute to a reduced patient-specific set of electrodes spread in four lobes (frontal, temporal, parietal, and occipital), as shown in Figure 6. The optimal number of electrodes is determined by a threshold sensitivity of 0.90. Table 6 and Figure 5 show the set of electrodes and its EEG scalp location for each subject according to the international 10–20 electrode position system. Sequential feature selection, a wrapped feature selection algorithm, is implemented for ranking the relevance of each electrode to yield the highest sensitivity when given as input to the MAML learning

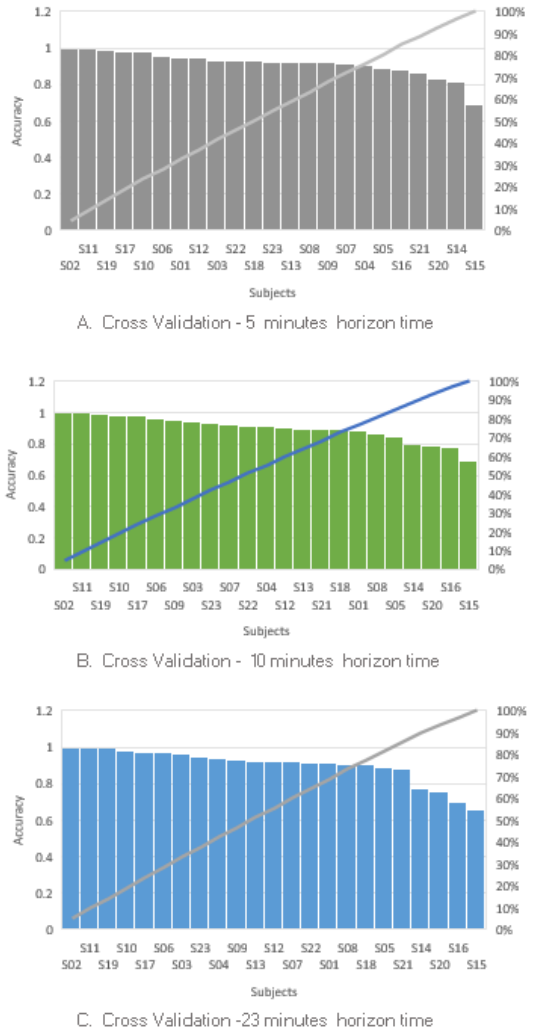

FIGURE 8. 10-fold cross-validation average score for each of the 23 subjects in the a) 5 horizon time, b) 10 horizon time, and c) 23 horizon time.

TABLE 5. Extracted features during the interictal frame of subject S_{01}.

Extracted Features	IMF_3	IMF_4	IMF_5
Maximum	45.972	30.850	29.906
Minimum	-81.192	-30.450	-29.639
Mean	0.52	-0.188	-0.118
Standard deviation	15.365	8.219	5.794
Coefficient of Var.	2923.1	-4349.2	-4900.4
Avg. PSD(V^2/Hz)	472.964	126.821	67.676

framework. Clearly, from Table 6, a specific reduced number of electrodes is attained for all 23 cases, in which the SFS algorithm is applied to the intrinsic functions extracted from the subject's 23 channels. The highest number of electrodes per subject is six, and the lowest number is two, representing a promising reduction scheme for wearable real-time seizure prediction. The MAML algorithm weight optimization process successfully learned the signature patterns of the IMFs and their PSD in the preictal and interictal transitions after 10 epochs, rendering a high optimized model for the 5 min, 23 min, and 30 min horizon times.

TABLE 6. Selected electrodes per subject.

Subject	Gender	No. of channels	Channels
S_{01}	M	5	FP1F7, F8T8, FP2F8, FP2F4, CZPZ
S_{02}	F	4	T7FT9, FZCZ, FT0T8, F7T7
S_{03}	M	6	FP1F3, F8T8, F3C3, FZCZ, C3P3, P8O2
S_{04}	F	4	FTT7, FP2F4, FP2F8, FT0T8
S_{05}	M	3	C3P3, P3O1, FP2F4
S_{06}	F	5	FP2F4, F4C4, C4P4, P4O2, FP2F8
S_{07}	M	3	C3P3, P3O1, FP2F4
S_{08}	F	5	FP2F4, F4C4, C4P4, P4O2, FP2F8
S_{09}	M	3	C3P3, P3O1, FP2F4
S_{10}	F	5	FP2F4, F4C4, C4P4, P4O2, FP2F8
S_{11}	M	5	F7T7, FP1F3, F4C4, P4O2, T8P8
S_{12}	F	4	F7T7, P4O2, T8P8, FT9FT10
S_{13}	M	4	FP1F7, F8T8, T8P8, P8O2
S_{14}	F	3	F7T7, T7P7, FT10T8
S_{15}	M	2	FP1F7, T7FT9
S_{16}	F	5	FP2F4, F4C4, C4P4, P4O2, FP2F8
S_{17}	M	4	P7O1, FP2F4, P4O2, F8T8
S_{18}	F	4	P7O1, FP2F4, P4O2, F8T8
S_{19}	M	6	F3C3, C3P3, FP2F4, C4P4, F8T8, FT9FT10
S_{20}	F	3	FP1F7, P8O2, T7FT9
S_{21}	M	4	P3O1, C4P4, P7T7, FT9FT10
S_{22}	F	5	FP1F7, F8T8, T8P8, P8O2, T7FT9
S_{23}	M	4	P3O1, FZCZ, P7T7, FT9FT10

To evaluate the classification performance of the MAML prediction model, we applied the measures of sensitivity, specificity, and the area under the ROC curve (AUC) to each of the 23 subjects testing data, as shown in Table 7. The performance of the MAML model tested in the female subjects scored similar sensitivity to that of the male subjects, as shown in Figure 7, and there is no significant difference in the gender groups since the p-value is not less than 0.05. The difference in the power spectral density of *IMFs* in the preictal and interictal segments is sustained across the 23 subjects with varying power levels and frequency distribution. In the training phase, these patterns are learned by the MAML-DNN combination to build a MAML model, which achieves an average sensitivity and specificity of 91% and 90%, respectively, in the testing phase.

A consistent accuracy score is established with the 10-fold cross-validation across all three horizon times. Figure 8 shows the 10-fold cross-validation average score for each subject in the 23 horizon time. The MAML prediction algorithm uses the second derivative to update the weight of the DNN. Once the model is trained and updated, a fast execution time in the testing phase is obtained. The false positive

TABLE 7. Prediction performance in three horizons.

	5 Min Horizon				10 Min Horizon				23 Min Horizon			
Subject	Sen	Spec	AUC	F1	Sen	Spec	AUC	F1	Sen	Spec	AUC	F1
S01	0.938	0.929	0.946	0.938	0.903	0.899	0.907	0.902	0.865	0.884	0.824	0.813
S02	0.870	0.900	0.785	0.757	0.913	0.706	0.810	0.827	0.890	0.900	0.785	0.757
S03	0.941	0.918	0.930	0.930	0.930	0.964	0.947	0.946	0.940	0.985	0.963	0.962
S04	0.857	0.924	0.891	0.887	0.906	0.951	0.928	0.926	0.896	0.983	0.940	0.937
S05	0.853	0.927	0.890	0.885	0.922	0.846	0.884	0.888	0.963	0.709	0.836	0.854
S06	0.940	0.989	0.965	0.964	0.939	0.986	0.963	0.962	0.939	0.986	0.963	0.962
S07	0.939	0.920	0.929	0.929	0.933	0.863	0.898	0.901	0.895	0.947	0.921	0.919
S08	0.880	0.910	0.785	0.757	0.913	0.796	0.810	0.827	0.890	0.900	0.785	0.757
S09	0.910	0.928	0.930	0.930	0.920	0.964	0.947	0.946	0.940	0.985	0.963	0.962
S10	0.941	0.919	0.930	0.931	0.904	0.932	0.918	0.916	0.938	0.953	0.945	0.945
S11	0.992	0.976	0.984	0.984	0.995	0.990	0.992	0.992	1.00	0.995	0.995	0.995
S12	0.918	0.951	0.934	0.933	0.942	0.898	0.920	0.921	0.872	0.955	0.914	0.910
S13	0.941	0.919	0.930	0.931	0.904	0.932	0.918	0.916	0.938	0.953	0.945	0.945
S14	0.806	0.852	0.829	0.825	0.872	0.751	0.811	0.822	0.900	0.627	0.763	0.791
S15	0.741	0.615	0.678	0.696	0.638	0.742	0.690	0.672	0.792	0.554	0.673	0.707
S16	0.941	0.919	0.930	0.931	0.904	0.932	0.918	0.916	0.938	0.953	0.945	0.945
S17	0.988	0.986	0.987	0.987	0.979	0.973	0.976	0.976	0.984	0.970	0.977	0.977
S18	0.745	0.985	0.864	0.845	0.965	0.905	0.935	0.937	0.982	0.889	0.936	0.938
S19	0.998	0.996	0.997	0.997	0.995	0.978	0.987	0.987	0.981	0.995	0.988	0.988
S20	0.876	0.745	0.811	0.820	0.771	0.868	0.820	0.809	0.557	0.885	0.721	0.665
S21	0.849	0.920	0.885	0.880	0.896	0.884	0.890	0.890	0.883	0.887	0.885	0.884
S22	0.961	0.867	0.914	0.917	0.951	0.881	0.916	0.918	0.938	0.940	0.939	0.938
S23	0.967	0.932	0.949	0.950	0.962	0.892	0.927	0.929	0.961	0.955	0.958	0.958

TABLE 8. Comparison with state-of-the-art epileptic seizure prediction methods.

Year	Authors	Classifying Algorithm	Dataset	Number of Channels	Patient-Specific Channels	Sen (%)	FPR (/h)	Horizon Time (min)
2017	Prathap *et al.* [41]	SPARSE	CHB	23	N0	86.11	-	-
2016	Cho *et al.* [38]	SVM	CHB	3	No	82.44	-	5
2020	Zhang *et. al.* [21]	CNN	CHB	18	No	92.2	0.12	30
2018	Truong *et al.* [42]	CNN	CHB	22	No	81.2	0.16	5
2017	Alotaiby *et al.* [43]	LDA	CHB	23	No	81	0.47	60
2020	Romney *et al.* [39]	DNN	CHB	2	No	86.7	0.27	23
2017	Chu *et al.* [44]	ATTRACTOR	CHB	-	No	86.77	0.367	55.3
2017	Birjandtalab *et al.* [45]	KNN	CHB	3	No	80.87	2.5	-
-	*Proposed Method*	MAML	CHB	(2,3,4,5,6,7)	Yes	92.31	0.26	23

rate per hour (FPR/h) for the three horizon times is shown in Figure 9. Most of the electrodes are located predominantly in the temporal lobes, as shown in Figure 6, which is consistent with the most frequent seizure types documented in the neurological literature. Electrodes located in the frontal-temporal brain area are the most significant for seizure prediction. The comparative study shown in Table 8 includes all the recent works implemented with reduced electrodes using the CHB-MIT database. The comparison shows that the proposed model with MAML surpasses similar studies in sensitivity and false positive rate performance measures. The proposed method yielded an average FPR/h of 0.26, which is among the lowest number obtained in recent seizure prediction research with any algorithm.

V. CONCLUSION

In this work, we present a MAML seizure prediction method with a patient-specific electrode channels selection. Our approach reduced the number of electrodes arranged on the scalp for each subject to pave the way toward real-time

seizure prediction with high sensitivity and specificity. The prediction model is built on patient-specific data using the model-agnostic meta-learning algorithm. The individual performance was validated using 10-F cross-validation. The reduced electrode-channel selection is sufficiently sensitive to capture or exclude patterns that lead to seizure prediction with varying horizon times. Patient-specific electrode reduction allowed us to train individual model for the subject's unique epileptiform EEG signals. Although the results look promising for wearable seizure prediction, the reduction of EEG channels should not be the preferred means to optimize EEG application in hospitals where all electrodes are required for accurate diagnosis. The performance measures of sensitivity, specificity, and FPR/h of the proposed model are encouraging. However, additional work is needed to implement the MAML model in a miniaturized device to test the sampled signal from the wireless scalp electrodes in real-time.

REFERENCES

[1] K. M. Fiest, K. M. Sauro, S. Wiebe, S. B. Patten, C.-S. Kwon, J. Dykeman, T. Pringsheim, D. L. Lorenzetti, and N. Jetté, "Prevalence and incidence of epilepsy," *Neurology*, vol. 88, no. 3, pp. 296–303, Jan. 2017, doi: 10.1212/WNL.0000000000003509.

[2] *The Economic Burden of Epilepsy in Australia, 2019–2020 | Epilepsy Foundation*. Accessed: Aug. 6, 2020. [Online]. Available: https://epilepsyfoundation.org.au/2020/02/08/the-economic-burden-of-epilepsy-in-australia-2019-2020/

[3] J. I. Sirven, "Epilepsy: A spectrum disorder," *Cold Spring Harbor Perspect. Med.*, vol. 5, no. 9, Sep. 2015, Art. no. a022848, doi: 10.1101/cshperspect.a022848.

[4] H. Khan, L. Marcuse, M. Fields, K. Swann, and B. Yener, "Focal onset seizure prediction using convolutional networks," *IEEE Trans. Biomed. Eng.*, vol. 65, no. 9, pp. 2109–2118, Sep. 2018, doi: 10.1109/TBME.2017.2785401.

[5] M. Zhou, C. Tian, R. Cao, B. Wang, Y. Niu, T. Hu, H. Guo, and J. Xiang, "Epileptic seizure detection based on EEG signals and CNN," *Frontiers Neuroinform.*, vol. 12, p. 95, Aug. 2018, doi: 10.3389/fninf.2018.00095.

[6] T. N. Alotaiby, S. A. Alshebeili, T. Alshawi, I. Ahmad, and F. E. A. El-Samie, "EEG seizure detection and prediction algorithms: A survey," *EURASIP J. Adv. Signal Process.*, vol. 2014, no. 1, pp. 1–21, Dec. 2014, doi: 10.1186/1687-6180-2014-183.

[7] P. A. Abhang, B. W. Gawali, and S. C. Mehrotra, "Technological basics of EEG recording and operation of apparatus," in *Introduction to EEG-and Speech-Based Emotion Recognition*. New York, NY, USA: Academic, 2016, pp. 19–50, doi: 10.1016/b978-0-12-804490-2.00002-6.

[8] V. Senger and R. Tetzlaff, "Cellular nonlinear network-based signal prediction in epilepsy: Method comparison," in *Proc. IEEE Int. Symp. Circuits Syst. (ISCAS)*, May 2015, pp. 397–400, doi: 10.1109/ISCAS.2015.7168654.

[9] H. Daoud and M. A. Bayoumi, "Efficient epileptic seizure prediction based on deep learning," *IEEE Trans. Biomed. Circuits Syst.*, vol. 13, no. 5, pp. 804–813, Oct. 2019, doi: 10.1109/TBCAS.2019.2929053.

[10] F. Samie, S. Paul, L. Bauer, and J. Henkel, "Highly efficient and accurate seizure prediction on constrained IoT devices," in *Proc. Design Autom. Test Eur. Conf. Exhib. DATE*, Jan. 2018, pp. 955–960, doi: 10.23919/DATE.2018.8342147.

[11] A. Kumar and S. Sharma, *Seizure, Complex Partial*. Treasure Island, FL, USA: StatPearls Publishing, 2018.

[12] C. Baumgartner, J. P. Koren, and M. Rothmayer, "Automatic computer-based detection of epileptic seizures," *Frontiers Neurol.*, vol. 9, p. 639, Aug. 2018, doi: 10.3389/fneur.2018.00639.

[13] A. H. Osman and A. A. Alzahrani, "New approach for automated epileptic disease diagnosis using an integrated self-organization map and radial basis function neural network algorithm," *IEEE Access*, vol. 7, pp. 4741–4747, 2019, doi: 10.1109/ACCESS.2018.2886608.

[14] E. B. Geller, T. L. Skarpaas, R. E. Gross, R. R. Goodman, G. L. Barkley, C. W. Bazil, M. J. Berg, G. K. Bergey, S. S. Cash, A. J. Cole, and R. B. Duckrow, "Brain-responsive neurostimulation in patients with medically intractable mesial temporal lobe epilepsy," *Epilepsia*, vol. 58, no. 6, pp. 994–1004, 2017, doi: 10.1111/epi.13740.

[15] N. Wang and M. R. Lyu, "Extracting and selecting distinctive EEG features for efficient epileptic seizure prediction," *IEEE J. Biomed. Health Inform.*, vol. 19, no. 5, pp. 1648–1659, Sep. 2015, doi: 10.1109/JBHI.2014.2358640.

[16] A. Ahmadi and H. Soltanian-Zadeh, "Epileptic seizure prediction using spectral entropy-based features of EEG," in *Proc. 4th Int. Conf. Pattern Recognit. Image Anal. (IPRIA)*, Mar. 2019, pp. 124–129, doi: 10.1109/PRIA.2019.8785984.

[17] J. G. Servin-Aguilar, L. Rizo-Dominguez, J. A. Pardinas-Mir, C. Vargas-Rosales, and I. Padilla-Cantoya, "Epilepsy seizure detection: A heavy tail approach," *IEEE Access*, vol. 8, pp. 208170–208178, 2020, doi: 10.1109/ACCESS.2020.3038397.

[18] I. Kiral-Kornek, S. Roy, E. Nurse, B. Mashford, P. Karoly, T. Carroll, D. Payne, S. Saha, S. Baldassano, T. O'Brien, and D. Grayden, "Epileptic seizure prediction using big data and deep learning: Toward a mobile system," *EBioMedicine*, vol. 27, pp. 103–111, Dec. 2017, doi: 10.1016/j.ebiom.2017.11.032.

[19] J. Kung, D. Kim, and S. Mukhopadhyay, "Adaptive precision cellular nonlinear network," *IEEE Trans. Very Large Scale Integr. (VLSI) Syst.*, vol. 26, no. 5, pp. 841–854, May 2018, doi: 10.1109/TVLSI.2018.2794498.

[20] H. Ghayab, Y. Li, S. Abdulla, M. Diykh, and X. Wan, "Classification of epileptic EEG signals based on simple random sampling and sequential feature selection," *Brain Informat.*, vol. 3, no. 2, pp. 85–91, 2016, doi: 10.1007/s40708-016-0039-1.

[21] Y. Zhang, Y. Guo, P. Yang, W. Chen, and B. Lo, "Epilepsy seizure prediction on EEG using common spatial pattern and convolutional neural network," *IEEE J. Biomed. Health Informat.*, vol. 24, no. 2, pp. 465–474, Feb. 2020, doi: 10.1109/JBHI.2019.2933046.

[22] A. Kumar and M. H. Kolekar, "Machine learning approach for epileptic seizure detection using wavelet analysis of EEG signals," in *Proc. Int. Conf. Med. Imag., m-Health Emerg. Commun. Syst. (MedCom)*, Nov. 2014, pp. 412–416, doi: 10.1109/MedCom.2014.7006043.

[23] A. Shahid, N. Kamel, A. S. Malik, and M. A. Jatoi, "Epileptic seizure detection using the singular values of EEG signals," in *Proc. ICME Int. Conf. Complex Med. Eng.*, May 2013, pp. 652–655, doi: 10.1109/ICCME.2013.6548330.

[24] A. S. Zandi, R. Tafreshi, M. Javidan, and G. A. Dumont, "Predicting epileptic seizures in scalp EEG based on a variational Bayesian Gaussian mixture model of zero-crossing intervals," *IEEE Trans. Biomed. Eng.*, vol. 60, no. 5, pp. 1401–1413, May 2013, doi: 10.1109/TBME.2012.2237399.

[25] Z. Zhang and K. K. Parhi, "Low-complexity seizure prediction from iEEG/sEEG using spectral power and ratios of spectral power," *IEEE Trans. Biomed. Circuits Syst.*, vol. 10, no. 3, pp. 693–706, Jun. 2016, doi: 10.1109/TBCAS.2015.2477264.

[26] M.-P. Hosseini, A. Hajisami, and D. Pompili, "Real-time epileptic seizure detection from EEG signals via random subspace ensemble learning," in *Proc. IEEE Int. Conf. Autonomic Comput. (ICAC)*, Jul. 2016, pp. 209–218, doi: 10.1109/ICAC.2016.57.

[27] P. Nejedly, J. Cimbalnik, P. Klimes, F. Plesinger, J. Halamek, V. Kremen, I. Viscor, B. H. Brinkmann, M. Pail, M. Brazdil, G. Worrell, and P. Jurak, "Intracerebral EEG artifact identification using convolutional neural networks," *Neuroinformatics*, vol. 17, no. 2, pp. 225–234, Apr. 2019, doi: 10.1007/s12021-018-9397-6.

[28] M. Eberlein, R. Hildebrand, R. Tetzlaff, N. Hoffmann, L. Kuhlmann, B. Brinkmann, and J. M'uller, "Convolutional neural networks for epileptic seizure prediction," in *Proc. IEEE Int. Conf. Bioinf. Biomed. (BIBM)*, Dec. 2018, pp. 2577–2582, doi: 10.1109/BIBM.2018.8621225.

[29] T. Hospedales, A. Antoniou, P. Micaelli, and A. Storkey, "Meta-learning in neural networks: A survey," 2020, *arXiv:2004.05439*.

[30] C. Lemke, M. Budka, and B. Gabrys, "Metalearning: A survey of trends and technologies," *Artif. Intell. Rev.*, vol. 44, no. 1, pp. 117–130, Jun. 2015, doi: 10.1007/s10462-013-9406-y.

[31] C. Finn, P. Abbeel, and S. Levine, "Model-agnostic meta-learning for fast adaptation of deep networks," 2017, *arXiv:1703.03400*.

[32] I. Sucholutsky and M. Schonlau, "'Less than one'-shot learning: Learning N classes from M<N samples," 2020, *arXiv:2009.08449*.

[33] *CHB-MIT Scalp EEG Database v1.0.0*. Accessed: Oct. 30, 2021. [Online]. Available: https://physionet.org/content/chbmit/1.0.0/

[34] J. B. Ali, N. Fnaiech, L. Saidi, B. Chebel-Morello, and F. Fnaiech, "Application of empirical mode decomposition and artificial neural network for automatic bearing fault diagnosis based on vibration signals," *Appl. Acoust.*, vol. 89, no. 3, pp. 16–27, Mar. 2015, doi: 10.1016/j.apacoust.2014.08.016.

[35] N. E. Huang, Z. Shen, S. R. Long, M. C. Wu, H. H. Shih, Q. Zheng, N. C. Yen, C. C. Tung, and H. H. Liu, "The empirical mode decomposition and the Hilbert spectrum for nonlinear and non-stationary time series analysis," *Proc. Roy. Soc. London A*, vol. 454, no. 1971, pp. 903–995, 1998, doi: 10.1098/rspa.1998.0193.

[36] Z. Wu and N. E. Huang, "Ensemble empirical mode decomposition: A noise-assisted data analysis method," *Adv. Adapt. Data Anal.*, vol. 1, no. 1, pp. 1–41, Jan. 2009, doi: 10.1142/S1793536909000047.

[37] A. Marcano-Cedeno, J. Quintanilla-Dominguez, M. G. Cortina-Januchs, and D. Andina, "Feature selection using sequential forward selection and classification applying artificial metaplasticity neural network," in *Proc. IECON 36th Annu. Conf. IEEE Ind. Electron. Soc.*, Nov. 2010, pp. 2845–2850, doi: 10.1109/IECON.2010.5675075.

[38] D. Cho, B. Min, J. Kim, and B. Lee, "EEG-based prediction of epileptic seizures using phase synchronization elicited from noise-assisted multivariate empirical mode decomposition," *IEEE Trans. Neural Syst. Rehabil. Eng.*, vol. 25, no. 8, pp. 1309–1318, Aug. 2017, doi: 10.1109/TNSRE.2016.2618937.

[39] A. Romney and V. Manian, "Comparison of frontal-temporal channels in epilepsy seizure prediction based on EEMD-ReliefF and DNN," *Computers*, vol. 9, no. 4, p. 78, Sep. 2020, doi: 10.3390/computers9040078.

[40] W. Zhao, W. Zhao, W. Wang, X. Jiang, X. Zhang, Y. Peng, B. Zhang, and G. Zhang, "A novel deep neural network for robust detection of seizures using EEG signals," *Comput. Math. Methods Med.*, vol. 2020, pp. 1–9, Apr. 2020, doi: 10.1155/2020/9689821.

[41] P. Prathap and T. A. Devi, "EEG spectral feature based seizure prediction using an efficient sparse classifier," in *Proc. Int. Conf. Intell. Comput., Instrum. Control Technol. (ICICICT)*, Jul. 2017, pp. 721–725, doi: 10.1109/ICICICT1.2017.8342653.

[42] N. D. Truong, A. D. Nguyen, L. Kuhlmann, M. R. Bonyadi, J. Yang, S. Ippolito, and O. Kavehei, "Convolutional neural networks for seizure prediction using intracranial and scalp electroencephalogram," *Neural Netw.*, vol. 105, pp. 104–111, Sep. 2018, doi: 10.1016/j.neunet.2018.04.018.

[43] T. N. Alotaiby, S. A. Alshebeili, F. M. Alotaibi, and S. R. Alrshoud, "Epileptic seizure prediction using CSP and LDA for scalp EEG signals," *Comput. Intell. Neurosci.*, vol. 2017, pp. 1–11, Jan. 2017, doi: 10.1155/2017/1240323.

[44] H. Chu, C. K. Chung, W. Jeong, and K.-H. Cho, "Predicting epileptic seizures from scalp EEG based on attractor state analysis," *Comput. Methods Programs Biomed.*, vol. 143, pp. 75–87, May 2017, doi: 10.1016/j.cmpb.2017.03.002.

[45] J. Birjandtalab, M. B. Pouyan, D. Cogan, M. Nourani, and J. Harvey, "Automated seizure detection using limited-channel EEG and non-linear dimension reduction," *Comput. Biol. Med.*, vol. 82, pp. 49–58, Mar. 2017, doi: 10.1016/j.compbiomed.2017.01.011.

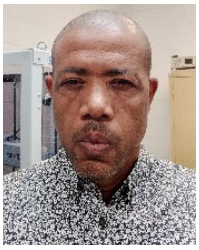

ANIBAL ROMNEY (Member, IEEE) received the M.S. degree in electrical engineering from the University of Puerto Rico at Mayagüez (UPRM), Mayagüez, PR, USA, where he is currently pursuing the Ph.D. degree in bioengineering. In 2012, he became a Full Professor at the University of Puerto Rico at Aguadilla. His research interests include machine learning, molecular biology, neuroscience, biosensors, and robotics. In 2001, he was awarded the NSF grant in communications and information technologies. As a Co-PI of a three-year project, he has enhance the preparation of underserved students for employment in the fields of manufacturing communications and information technologies industries.

VIDYA MANIAN (Member, IEEE) received the Ph.D. degree in computing, information science, and engineering from the University of Puerto Rico at Mayagüez (UPRM), Mayagüez, PR, USA, in 2004. She was a Visiting Scholar with the Lane Department of Computer Science and Electrical Engineering, West Virginia University, Morgantown, WV, USA. In 2005, she was a Postdoctoral Associate in electrical and computer engineering (ECE) at UPRM. In 2006, she joined at UPRM, as an Assistant Professor in ECE. She is currently a Professor in ECE with UPRM, and the Director of the Brain–Computer Interface Laboratory. Her research interests include multispectral image processing, bioengineering, bio-sensory data fusion, neuroscience, and machine learning. In 2013, the First Lady of Puerto Rico recognized Dr. Manian for her outstanding contribution to education and research.